to note that even before ion ejection the FTMS spectra seem to have a significantly lower level of low-mass matrix-related background peaks than when the same sample is run on a sector mass spectrometer (VG 7070). One possible reason for this difference is that the time scale of mass analysis by FTMS is many milliseconds compared to only microseconds for a sector mass spectrometer. As a result, matrix-related ions may be less abundant in the FTMS spectra because they undergo metastable decay before they are detected. Another possible explanation is that the pulsed cesium ion beam used in our experiments causes less radiation damage of the glycerol than the continuous FAB beam used with sector instruments.[41]

Acknowledgment. Financial support by the National Institutes of Health (GM34327) is gratefully acknowledged. C.B.L. gratefully acknowledges support as a postdoctoral fellow from the University of California President's Fellowship Program, and T.J.M. was supported by a REU grant from the National Science Foundation. We also wish to thank Gary Look for assistance with the UV/Vis spectra of the peptides.

Registry No. Val-Ala-Ala-Phe, 21957-32-4; Met-Arg-Phe-Ala, 67368-29-0; gramicidin S, 113-73-5.

(41) Dass, C.; Desiderio, D. M. *Anal. Chem.* **1988**, *60*, 2723-2729.

X-14885A: An Ionophore Closely Related to Calcimycin (A-23187). NMR, Thermodynamic, and Kinetic Studies of Cation Selectivity

A. M. Albrecht-Gary,*,† S. Blanc-Parasote,† D. W. Boyd,† G. Dauphin,§ G. Jeminet,*,§ J. Juillard,‖ M. Prudhomme,§ and C. Tissier‖

Contribution from the Laboratoire de Chimie Physique et d'Electroanalyse, U.A. 405 CNRS, EHICS, Université Louis Pasteur, 67000 Strasbourg, France, Laboratoire de Chimie Organique Biologique, U.A. 485 CNRS, and Laboratoire des Interactions Solutés-Solvants, U.A. 434 CNRS, Université Blaise Pascal, 63170 Aubière, France. *Received October 20, 1988*

Abstract: X-14885A is an open-chain carboxylic ionophore, recently isolated from a *Streptomyces* strain. NMR data have shown that the free acid form adopts a pseudocyclic conformation in chloroform, while in the neutral A_2Mg complex a rotation of the benzoxazole arm is achieved to accommodate the cation in a sandwich system. The replacement of the -NHMe by an -OH function and of a methyl group by H in position 15 for X-14885A does not lead to a large modification in the conformation of the new microbial metabolite in solution. The acid-base equilibria and the thermodynamics of association with alkali and alkali-earth cations are determined in methanol, from potentiometric and spectrophotometric measurements. Divalent cations M^{2+} form strong complexes of 1:1 (AM^+) and 2:1 (A_2M) stoichiometries, following the sequence $Ca^{2+} > Mg^{2+} > Sr^{2+} > Ba^{2+}$. For $AM^+ + A^- \rightleftarrows A_2M$, log K_{A_2M} are, respectively, 8.0, 7.3, 6.9, and 6.2 ($I = 0$). A complete kinetic study is carried out in methanol for the A_2Mg and A_2Ca complexes, with use of a stopped-flow system. This work shows that the rate-limiting steps of the formation and dissociation mechanisms are associated with the charged complex AM^+, the addition or loss of the second ligand being faster. As for the closely related ionophore A-23187 (calcimycin), the selectivity calcium/magnesium has predominantly a kinetic origin, with faster formation and dissociation rates of the calcium complexes. The replacement of the -NHMe group in calcimycin by an -OH group in X-14885A has a drastic effect in the acid-base properties of X-14885A and on the acid-catalyzed dissociation pathway of its complexes.

In the growing class of carboxylic polyether ionophores isolated from bacterial strains,[1] A-23187 or calcimycin[2] (Figure 1a) occupies an unusual place as a carrier for divalent cations, especially calcium.[3] Owing to its ability to modify intracellular calcium concentration,[4] it is one of the most frequently quoted chemicals in the biochemical literature. A great number of biological events have been shown to be modified by addition of this ionophore; among them can be cited induction of leucotrienes[5] and interferon[6] production.

The overall transport mechanism in the membrane is an electroneutral exchange[7] of an M^{2+} for $2H^+$, and rate constants for the different steps in the diffusion process have been studied in model phospholipid membranes.[8]

Our general purpose was to understand the formation and dissociation of the neutral lipophilic complex, A_2M (2:1 ligands/cation), which diffuses through the membrane and is responsible for the capture and liberation of the divalent cations at the water/membrane interface. In previous work,[9,10] the thermodynamics of calcimycin complexation by alkali-metal and alkaline-earth cations was studied in methanol or methanol/water systems. Complexation and decomplexation kinetics were also

† Laboratoire de Chimie Physique et d'Electroanalyse, Université Louis Pasteur de Strasbourg.
§ Laboratoire de Chimie Organique Biologique, Université Blaise Pascal.
‖ Laboratoire des Interactions Solutés-Solvants, Université Blaise Pascal.

(1) Westley, J. W. In *Polyether Antibiotics, Naturally Occurring Ionophores*; Westley, J. W., Ed.; Marcel Dekker: New York, 1982; Vol. I, pp 1-41.
(2) (a) Hamill, R. L.; Gorman, M.; Gale, R. M.; Higgens, C. E.; Hoehn, M. M. Proceedings 12th Interscience Conference on Antimicrobial Agents and Chemotherapy, Atlantic City, NJ, 1972. (b) Chaney, M. O.; Demarco, P. V.; Jones, N. D.; Occolowitz, J. L. *J. Am. Chem. Soc.* **1974**, *96*, 1932.
(3) (a) Reed, P. W.; Lardy, H. A. *J. Biol. Chem.* **1972**, *247*, 6970. (b) Pfeiffer, D. R.; Lardy, H. A. *Biochemistry* **1976**, *15*, 935. (c) Pfeiffer, D. R.; Hutson, S. M.; Kauffman, R. F.; Lardy, H. A. *Ibid.* **1976**, *15*, 2690.
(4) Reed, P. W. In *Polyether Antibiotics, Naturally Occurring Ionophores*; Westley, J. W., Ed.; Marcel Dekker: New York, 1982; Vol. I, pp 185-302.
(5) Samuelsson, B. *Angew. Chem., Int. Ed. Engl.* **1983**, *22*, 805.
(6) Braude, I. A.; Tarr, C. *Methods Enzymol.* **1986**, *119*, 72.
(7) Pfeiffer, D. R.; Taylor, R. W.; Lardy, H. A. *Ann. N. Y. Acad. Sci.* **1978**, *307*, 402.
(8) Kolber, M. A.; Haynes, D. H. *Biophys. J.* **1981**, *36*, 369.
(9) (a) Tissier, C.; Juillard, J.; Dupin, M.; Jeminet, G. *J. Chim. Phys.* **1979**, *76*, 611. (b) Tissier, C.; Juillard, J.; Boyd, D. W.; Albrecht-Gary, A. M. *J. Chim. Phys.* **1985**, *82*, 899.
(10) Chapman, C. J.; Puri, A. K.; Taylor, R. W.; Pfeiffer, D. R. *Biochemistry* **1987**, *26*, 5009.

0002-7863/89/1511-8598$01.50/0

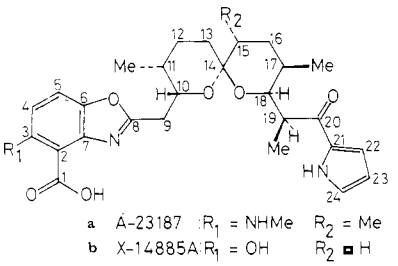

Figure 1. Chemical structures of: (a) A-23187 (calcimycin), R_1 = NHMe, R_2 = Me; (b) X-14885A, R_1 = OH; R_2 = H.

determined in the same media.[11,12] In addition, analogues of calcimycin with modified benzoxazole ring substituents were characterized in a biphasic model system.[13] It has appeared that an electron-donating substituent in the 3-position (Figure 1) and hydrogen bonding to the carboxyl group are essential for the formation of stable neutral complex A_2M. These observations were corroborated by ab initio computations.[14]

Recently, a novel bacterial ionophore X-14885A (Figure 1b) was isolated,[15] with a molecular structure closely resembling that of calcimycin. The differences are that an -OH group replaces the $-NHCH_3$ on the benzoxazole ring and a methyl group is missing in the 15 position. The selectivity of transport determined by the U-tube system and labeled cations was $Mg^{2+} > Ca^{2+}$,[15] the opposite of calcimycin. This new compound[15] gives us the opportunity to examine how the recognition of cations, especially calcium and magnesium, is affected by the two structural changes on the benzoxazole ring and the spiroketal moiety. We present here NMR, thermodynamic, and kinetic studies of cation complexation by this new compound.

Experimental Section

(1) A-23187 (Calcimycin) and X-14885A Productions. A-23187 was obtained from the strain *Streptomyces chartreusis* NRRL 3882, following a fermentation process already described.[9]

Antibiotic X-14885A was also prepared by fermentation, using the deposit strain of *Streptomyces sp.* 12350. Composition of the inoculum medium was (in g/L, tap water) as follows: tomato pomace, 5.0; soyoptim (SIO, 62150 Saint-Laurent Blangy), 5.0; peptone I.B.F. (Pointet-Girard, 92320 Villeneuve-La-Garenne), 5.0; yeast extract (Difco, Detroit, MI), 5.0; maltodextrin 0.3 (Roquette, 62136 Lestrem), 20; glucose, 5.0; K_2HPO_4, 1.0; $CoSO_4$, 0.01; $CaCO_3$, 1.0. The pH was adjusted to 7.0 before sterilization. The inoculated flask was put on a rotary shaker (205 rpm) at 28 °C for 72 h. The resulting culture (100 mL) was used to inoculate 1 L of the same medium in a 2-L fermentor. This second seed stage was incubated at 28 °C for 24 h. The whole culture was transferred to inoculate 15 L of the following medium, in a 20-L fermentor (in g/L, tap water): glucose, 25, soyase, BBL (Biomérieux, 69752 Charbonnière-les-Bains), maltodextrin (Roquette), 20; soyoptim (SIO), 5.0; cornsteep solid (Roquette), 5.0; $CaCO_3$, 2.5; $CoSO_4$, 0.01. The pH was adjusted to 7.2 with NaOH. The fermentation was carried out at 28 °C for 192 h. Isolation of antibiotic X-14885A was made following the process described by the Hoffmann-La Roche group.[16] About 2 g of pure compound were obtained, identical (TLC, UV, IR, NMR, mass spectrum) to a sample provided by Hoffmann-La Roche.

(2) NMR Measurements. ^1H and ^{13}C NMR spectra were recorded on a Bruker WM 400 or on a Bruker MSL 300. The concentrations of antibiotic used were about 5×10^{-2} mol L^{-1}. The applied pulse sequence was $(\pi/2)-(t_1)-(\pi/4)-(\text{FID}, t_2)$ for ^1H COSY spectra. For $^1H-^{13}C$ shift correlations, the applied pulse sequence was $(\pi/2, {}^1H)-(t_1/2)-(\pi, {}^{13}C)-(t_1/2)-(\tau_1)-(\pi/2, {}^1H; \pi/2, {}^{13}C)-(\tau_2)-(\text{BB}, {}^1H; \text{FID}, t_2)$ with τ_1 = 0.003 57 s and τ_2 = 0.001 785 s. For $J-\delta(^1H)$ correlation, the applied pulse was $(\pi/2)-(t_1/2)(\pi)-(t_1/2)-(\text{FID}, t_2)$.

Ionophores A-23187 (Calcimycin) and X-14885A in CD_3OD. Selective irradiations and $J-\delta$ correlation were performed at 400.13 MHz. For $J-\delta$ correlation, the spectral width in F_2 was 4000 Hz and in F_1 62.5 Hz. The number of data points in F_2 was 4096, and 64 increments were recorded (NS = 32). Before Fourier transformation, the data were multiplied with sine bell shifted $\pi/2$ in each dimension. Selective irradiations were performed on a Bruker MSL 300 operating at 300.13 MHz for the ^1H NMR spectrum of the ionophore X-14885A in CD_3OD.

Ionophore X-14885A in $CDCl_3$. The COSY ^1H spectrum of the free ionophore AH was recorded in $CDCl_3$. The spectral widths in F_1 and F_2 were 3200 Hz. The number of data points in t_2 was 2048, and 512 increments were performed (NS = 64). Before Fourier transformation and symmetrization, the data were multiplied with unshifted sine bell. The $\pi/2$ pulse was 12 μs. ^{13}C spectra were recorded at 100 MHz.

Neutral $(X-14885A)_2$ Mg Complex in $CDCl_3$. The COSY ^1H spectrum (400.13 MHz) of the neutral A_2Mg complex was recorded in $CDCl_3$. The spectral widths in F_1 and F_2 were 3086 Hz; the number of data points in t_2 was 2048, and 256 increments were performed (NS = 32). Before Fourier transformation and symmetrization, the data were multiplied with unshifted sine bell. The $\pi/2$ pulse was 12 μs. ^{13}C spectra were recorded at 100 MHz. A composite pulse is used for the J-modulated spin-echo spectrum.

$^1H-^{13}C$ shift correlations (Bruker AM 400) were determined using a spectral width of 3086 Hz in F_1 and of 17 857 Hz in F_2. The number of data points in t_2 was 2048, and 512 increments were performed (NS = 80). Before Fourier transformation, the data were multiplied with unshifted sine bell in F_2 and exponential in F_1. The $\pi/2$ pulse was 7.5 μs for ^{13}C and the decoupler $\pi/2$ pulse was 10 μs. For $^1H-^{13}C$ "long range" shift correlation, the parameters were identical with those used for $^1H-^{13}C$ shift correlation except for the spectral width (19 230 Hz in F_2, τ_1 = 0.08 s and τ_2 = 0.04 s, NS = 128).

(3) Potentiometric and Spectrophotometric Measurements. Complexation of all alkali and alkaline-earth cations by X-14885A has been studied in pure methanol using potentiometry. In order to know the corresponding stability constants in the conditions of the kinetic experiments, complexation of calcium and magnesium cations by the ionophore has also been studied in a 0.1 mol L^{-1} solution of tetrabutylammonium perchlorate (Fluka, purum) in methanol using a procedure combining spectrophotometric measurements and potentiometric determination of $-\log [H^+]$. Both types of experiments were done at 25.0 °C using appropriate cells. Solvent used was an anhydrous methanol, which contained less than 0.01% of water (Merck, waterfree). Metal cations were introduced as perchlorates, which were previously dried in a vacuum oven at 60 °C. In the case of alkaline-earth perchlorates, constitutive water was not removed and the solutions in methanol were titrated using disodium salt of EDTA and murexide.

Potentiometric measurements were done using a calomel reference electrode, in methanol with a junction made of a 0.08 mol L^{-1} tetraethylammonium perchlorate solution in methanol and as indicator electrodes either a H^+ glass electrode (Tacussel, High Alcalinity) alone or, in the case of some cations, two glass electrodes, one specific for H^+, the other one specific for Na^+ (Beckman 39278), K^+, or Rb^+ (Beckman general cationic 39137). Buffer solutions proposed by De Ligny et al.[17] were used for standardization. Potentiometric measurements were recorded with either Orion 701 A or Tacussel Aries 10000 millivoltmeters. Stability constants were obtained using a method previously described;[9a,18] it consisted of measuring the $-\log [H^+]$ values and eventually the $-\log [M^+]$ values ($M = Na^+$, K^+, or Rb^+) during the titration of an ionophore acid solution, in the presence of the metal perchlorate, by a tetrabutylammonium methoxide solution. The data were processed either using a Bjerrum formation function[9] for ordinary titrations or using a Leden formation function for titrations monitored by two sensitive electrodes.[18] This last procedure allows the activities of both the hydrogen ions and the metal cations to be followed along the titration curves.

The change of the UV-visible absorption spectra as a function of the hydrogen ion concentration was recorded on a Cary 17-D spectrophotometer, coupled by a digital interface to a Periferic Zip 30 printer. Ionophore solutions, in the presence or absence of an alkaline-earth cation, were acidified with $HClO_4$ (Merck, per analysis, 70%) up to 3×10^{-3} mol L^{-1}, and tetrabutylammonium methoxide (Merck, 25% in methanol) was added progressively. A small sample (500 μL) was taken after each addition in order to record the UV-visible spectrum. The -log

(11) Krause, G.; Grell, E.; Albrecht-Gary, A. M.; Boyd, D. W.; Schwing, J. P. In *Physical Chemistry of Transmembrane Ion Motions*; Spach, G., Ed.; Elsevier: Amsterdam, The Netherlands, 1983; pp 255-263.
(12) Thomas, T. P.; Pfeiffer, D. R.; Taylor, R. W. *J. Am. Chem. Soc.* **1987**, *109*, 6670.
(13) Prudhomme, M.; Dauphin, G.; Jeminet, G. *J. Antibiot.* **1986**, *39*, 922.
(14) Gresh, N. *Nouv. J. Chim.* **1986**, *10*, 201.
(15) (a) Liu, C. M.; Chin, M.; Prosser, B. La. T.; Palleroni, N. J.; Westley, J. W.; Miller, P. A. *J. Antibiot.* **1983**, *36*, 1118. (b) Westley, J. W.; Liu, C. M.; Blount, J. F.; Sello, L. M.; Troupe, N.; Miller, P. A. *J. Antibiot.* **1983**, *36*, 1275.
(16) Liu, C. M.; Tresner, H. D.; Westley, J. W. U.S. Patent 4,352,934, 1982.
(17) De Ligny, C. L.; Luykx, P. F. M.; Rehbach, M.; Wieneke, A. A. *Rec. Trav. Chim. Pays-Bas* **1960**, *79*, 699.
(18) Pointud, Y.; Tissier, C.; Juillard, J. J. *Solution Chem.* **1983**, *12*, 473.

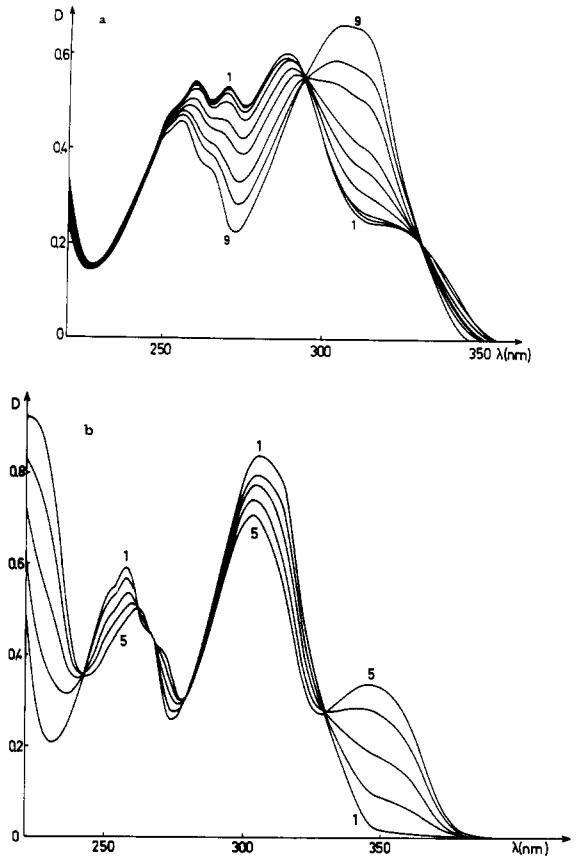

Figure 2. Evolution of the absorption spectra as a function of hydrogen ion concentrations. (a) [X-14885A] = 1.7×10^{-4} mol L^{-1}, [Mg^{2+}] = 1.42×10^{-3} mol L^{-1}. Spectra (−log [H^+]): 1 (3.54), 2 (3.71), 3 (3.84), 4 (4.07), 5 (4.28), 6 (4.45), 7 (4.75), 8 (5.03), 9 (7.24). (b) [X-14885A] = 2.0×10^{-4} mol L^{-1}, [Ca^{2+}] = 3.5×10^{-2} mol L^{-1}. Spectra (−log [H^+]): 1 (9.97), 2 (11.09), 3 (11.57), 4 (12.04), 5 (12.55). Solvent, methanol; I = 0.1; T = 25.0 ± 0.1 °C; optical length, 2 mm.

[H^+] values were measured with a combined glass electrode (Tacussel, High Alcalinity), in which the reference electrode (Ag/AgCl) was filled with tetrabutylammonium chloride (5×10^{-2} mol L^{-1}) and tetrabutylammonium perchlorate (5×10^{-2} mol L^{-1}) in methanol. Potential differences were measured with a Tacussel Isis 20000 millivoltmeter. The spectrophotometric and potentiometric data obtained were treated by the program LETAGROP-SPEFO,[19] which uses a nonlinear least-squares method in order to determine the thermodynamic constants and the corresponding absorption spectra of the different species. The range of −log [H^+] used in the experiments concerning the protolytic species of the free ionophore X-14885A was from 3.1 to 12.3. Similar experiments were done with calcium or magnesium present: absorption spectra were taken (220–350 nm) covering a range of −log [H^+] from 3.3 to 8.0 and using different ionophore/cation stoichiometries. For each cation, a metal concentration in excess (10–50-fold) with respect to the ionophore concentration (about 2×10^{-4} mol L^{-1}) was chosen for the titration. The latter was also carried out with the stoichiometry 2:1 ionophores/cation. An example of the evolution of the absorption spectra as a function of hydrogen ion concentrations is given in Figure 2a.

In more basic conditions (9 < −log [H^+] <13), the acid–base titration in presence of calcium or magnesium shows the appearance of new complexed species (Figure 2b), which were not observed with A-23187 in similar experimental conditions. These species are characterized by a decrease of the absorbance at 310 nm and by the presence of an absorption maximum at 345 nm.

(4) Kinetic Measurements. The formation and dissociation reactions of alkaline-earth cations with the ionophore X-14885A in methanol involve fast reaction kinetics, requiring for their study a stopped-flow technique. We used a Durrum-Gibson D-110 instrument spectrophotometer connected to a Tektronix Q-11 fast-storage oscilloscope; the signal could also be digitized and stored using a Datalab DL 905 transient recorder. An on-line Apple II microcomputer was programmed to treat first-order or pseudo-first-order kinetics.[20] From our thermodynamic studies and with the help of the program HALTAFALL,[21] it was possible to calculate very accurate experimental conditions for the kinetic experiments. Basic conditions for the preparation of the complexes were obtained using tetrabutylammonium methoxide. The autoprotolytic constant of methanol[17] at 25.0 °C and I = 0.1 is 16.7, so that a concentration of 10^{-5} mol L^{-1} in tetrabutylammonium methoxide ensures a hydrogen concentration of less than 10^{-11} mol L^{-1}. Acidic conditions, from 10^{-2} to 3×10^{-5} mol L^{-1} in hydrogen ion, were necessary for the complete dissociation of the complexes. For concentrations of hydrogen ion greater than 2.5×10^{-4} mol L^{-1}, perchloric acid solutions in methanol were employed. For hydrogen ion concentrations between 2.5×10^{-4} and 3×10^{-6} mol L^{-1}, we used dichloroacetic acid (BDH Laboratory Reagents) partially neutralized by tetrabutylammonium methoxide as a buffer solution.[53] The dissociation kinetics experiments were carried out with hydrogen ion concentrations, which could be considered constant during the reaction. That is true either for the buffer solutions or for perchloric acid solutions in at least 10-fold excess of the complex concentration.

We chose to study the second-order stoichiometric formation of the neutral A_2M (2:1 ionophores/cation) complexes, because the reactions were too fast to be studied in pseudo-first-order conditions. The antibiotic X-14885A solutions were prepared so as to give a concentration of 3.0×10^{-5} mol L^{-1} after mixing, and the solutions of alkaline-earth cations were prepared so as to give a corresponding concentration of 1.5×10^{-5} mol L^{-1}. The range of hydrogen ion considered was from 10^{-7} to 10^{-9} mol L^{-1}; an imidazole (Merck, purum) buffer was used in these conditions.

Table I. Proton NMR Chemical Shifts (ppm, Internal TMS)[a]

protons	free ionophores: X-14885A in $CDCl_3$	free ionophores: X-14885A in CD_3OD	free ionophores: A-23187 in CD_3OD	X-14885A neutral A_2Mg complex in $CDCl_3$
OH	10.90			14.1
NHpy	9.62	11.1[b]		12.9
5	7.70	7.85	7.75	7.50
24	7.07	7.04	7.01	7.30
22	6.93	6.88	6.89	6.90
4	7.01	6.95	6.73	7.00
23	6.26	6.17	6.19	6.25
10	4.30	4.08	4.17	3.95
18	3.62	3.35	3.38	2.50
19	3.23	3.18	3.19	3.00
9(pro-*S*)	3.17	3.06	3.05	2.75
9(pro-*R*)	3.05	2.92	2.92	2.78
CH_3–N			2.99	
13Aa[c]	1.51	1.53	1.77	1.33
17	1.65	1.75	1.55	1.15
16Aa	1.95	1.90	1.58	1.37
15a	1.60[c]	1.46	1.58	1.15
	1.44[d]	1.41		1.15
11	1.58	1.48	1.55	1.83
12Aa	1.49	1.42	1.41	1.00
16Be[d]	1.40	1.32	1.24	1.25
12Be	1.30	1.20	1.13	0.83
13Be	1.17	1.14	0.97	1.07
$Me_{15'}$			0.88	
$Me_{11'}$	0.96	0.96	0.97	0.85
$Me_{17'}$	0.99	0.94	0.95	0.76
$Me_{19'}$	0.96	0.77	0.80	0.75

[a] A and B refer respectively to the protons at lowest and highest field. [b] Partially exchanged. [c] a = axial protons. [d] e = equatorial protons.

Results

(1) NMR Assignments. NMR spectra have been recorded for X-14885A in $CDCl_3$ and CD_3OD and for A-23187 in CD_3OD. Special attention was devoted to the magnesium complex A_2M. Assignment of the ^1H (performed at 400 MHz) and ^{13}C (100 MHz) resonances for this neutral magnesium complex was carried out by using 2D NMR methods, in several "steps", following a strategy previously described.[22] The results are presented in Tables I and II.

(19) Sillen, L. G.; Warnqvist, B. *Ark. Kemi* **1968**, *31*, 315 and 377.

(20) Lagrange, J.; Lagrange, P. *J. Chim. Phys.* **1984**, *81*, 425.

(21) Ingri, N.; Kakolowicz, W.; Sillen, L. G.; Warnqvist, B. *Talanta* **1967**, *14*, 1261.

(22) Beloeil, J. C.; Delsuc, M. A.; Lallemand, J. Y.; Dauphin, G.; Jeminet, G. *J. Org. Chem.* **1984**, *49*, 1797.

Table II. ^{13}C NMR Chemical Shifts of the Free Ionophore X-14885A and of Its Neutral Magnesium Complex in $CDCl_3$ (ppm, Internal TMS)

carbon atoms	free ionophore X-14885A	X-14885A neutral A_2Mg complex	carbon atoms	free ionophore X-14885A	X-14885A neutral A_2Mg complex
17′	10.6	9.6	2	101.8	106.7
11′	10.9	10.9	23	110.3	111.0
19′	13.2	11.4	5	114.7	114.6
13	29.6	29.4	4	116.5	115.2
12	25.7	25.1	22	117.5	121.2
17	27.0	26.0	24	124.4	128.6
11	29.3	28.8	21	133.1	133.7
15	26.1	26.1	6	140.2	138.8
16	29.5	29.1	7	143.2	142.7
9	32.7	32.2	3	159.7	160.7
19	42.6	42.8	8	168.1	170.4
10	68.8	72.0	1	169.5	172.4
18	73.3	75.1	20	194.0	196.1
14	96.5	96.2			

The ^1H–^1H COSY homonuclear shift 2D experiments[23,24] gave a partial assignment of the systems. Coupled protons H_4 and H_5 on the COSY spectrum were assigned by comparison with the corresponding resonances for the homologue magnesium complex formed with calcimycin[25] and correction for substituent effects.[26] Likewise, positions of protons H_{23}, H_{24}, and H_{25} of the pyrrole ring were found unmodified as compared to calcimycin spectra.[27,28] The NH pyrrole signal was identified by homonuclear decoupling. Two groups of protons $H_{12A,B}$, $H_{13A,B}$ and $H_{15A,B}$, $H_{16A,B}$ remained unassigned with possibilities of inversion within these groups. 1D ^{13}C spectra analysis (BB and J-modulated spin–echo), together with ^1H–^{13}C heteronuclear shift-correlated 2D experiments,[23,29] allowed a partial assignment of ^{13}C resonances. ^{13}C–^1H correlations for C_{12}, C_{13}, C_{15}, and C_{16} gave the assignment of the four carbon–proton pairs. Quaternary carbons C_1, C_2, C_3, C_6, C_7, C_8, C_{14}, C_{20}, and C_{21} were identified through their relation with a distant proton, by a long-range shift correlation,[23] with experimental conditions providing enhancement of the signal of carbons weakly coupled to protons (J = 6 Hz). The following $^2J_{C,H}$ and $^3J_{C,H}$ correlations were pointed out: C_2–H_4, C_3–H_5, C_6–H_5, C_8–H_9, Me_{11}–H_{10}, $Me_{19'}$–$H_{19'}$, C_{20}–$Me_{19'}$. Remaining resonances at 96.2, 133.7, 142.7, and 172.4 ppm were assigned, respectively, to C_{14},[30] C_{21}, C_7, and C_1.[30]

The complete assignment of the ionophore X-14885A, in the acid form, for ^1H and ^{13}C resonances in $CDCl_3$ was deduced from the COSY ^1H–^1H spectrum, from the J-modulated spin–echo ^{13}C spectrum, which gave multiplicity of ^{13}C signals, and by comparison with the magnesium complex resonances for quaternary carbons. For A-23187 (calcimycin) and X-14885A in CD_3OD, ^1H and ^{13}C 1D spectra, homonuclear decoupling, and chemical shift similarities with $CDCl_3$ permitted complete assignment.

Coupling constants ^1H–^1H gathered in Table III were measured directly from the spectra taken in $CDCl_3$ and in CD_3OD. An additional 2D J–δ ^1H–^1H spectrum was also used for A-23187 (calcimycin) in CD_3OD.

(2) Thermodynamics and Electronic Spectra. (a) Ionophore X-14885A in Methanol. We have gathered in Table IV the pK values determined for the dissociation of the protonated sites of the free ionophore X-14885A in pure methanol. These data have been compared to the corresponding ones obtained in the same conditions for calcimycin.[9,11]

Table III. Apparent Coupling Constants (Hz) of the Free Ionophores, Calcimycin and X-14885A, and of X-14885A Neutral Magnesium Complex[a]

protons	free ionophores: X-14885A in $CDCl_3$	free ionophores: X-14885A in CD_3OD	free ionophores: A-23187 in CD_3OD	X-14885A neutral A_2Mg complex in $CDCl_3$
4–5	9.0	9.0	9.1	9.0
10–9A	9.0	11.0	10.0	11.25
10–9B	6.0	4.0	4.0	3.25
10–11	2.0	2.0	2.0	2.0
16A–16B	13.5	13.5		13.5
12A–12B		13.0		13.5
13A–13B		13.5		13.0
9A–9B	15.0	14.0	14.0	13.0
15A–15B	14.0			
19–18	10.0	10.0	10.0	10.0
18–17	2.0	2.0	2.0	1.5
11–12Aa	d		4.0	3.0
11–12Be	d	2.0	2.0	2.0
12Aa–13Aa	d	12.0	13.0	13.0
12Aa–13Be	d	3.5	4.0	4.0
12Be–13Aa	d	4.5	4.5	4.5
12Be–13Be	d	2.0	2.5	2.0
17–16Aa	5.0	5.0	d	5.0
17–16Be	2.0			2.0
16a–15Aa	13.5	13.5	d	d
16Be–15Be	d			
16Be–15Aa	4.0			d
16Aa–15Be	5.0	5.0	d	d
19–$Me_{19'}$	6.9	7.0	7.0	7.0
15–$Me_{15'}$			5.0	
17–$Me_{17'}$	7.0	7.0	7.0	7.0
11–$Me_{11'}$	7.0	7.0	7.0	7.0

[a] d = degenerated.

Table IV. pK_1 and pK_2 Values Determined for the Ionophores X-14885A and A-23187 (Calcimycin)[9,11] in Pure Methanol

equilibrium	X-14885A	A-23187
$AH \overset{K_1}{\rightleftharpoons} A^- + H^+$	8.42 ± 0.02^a 7.6 ± 0.1^b	10.94 ± 0.02^a 10.4 ± 0.1^b
$AH_2^+ \overset{K_2}{\rightleftharpoons} AH + H^+$	2.34 ± 0.05^a 2.3 ± 0.8^b	3.12 ± 0.05^a 3.3 ± 0.2^b

[a] From potentiometric measurements; I = 0. [b] From simultaneous potentiometric and spectrophotometric measurements; I = 0.1. T = (25.0 ± 0.1) °C.

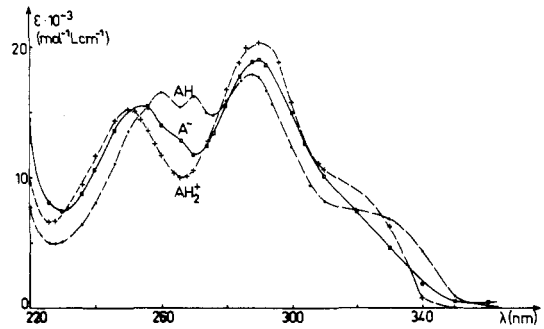

Figure 3. Electronic spectra of the deprotonated species and of the protonated forms of the free ionophore X-14885A in methanol.

Calcimycin and X-14885A were found to have very different pK_1 values (for the carboxyl group) as expected from the pK values obtained for model acids: 7.8 for salicylic acid as compared to 9.8 for anthranilic acid and 9.7 for its N-methyl derivative. A pK_1 difference of 2.4 between the two ionophores is in good agreement with a pK_1 difference of 1.9 between the model acids. This difference may be attributed to the absence of hydrogen bonding of the carboxyl group to the oxazolic nitrogen in the model acids.

A lower pK_2 value was determined (2.3 from potentiometric measurements and the same value from simultaneous potentio-

(23) Bax, A. *Two-Dimensional Nuclear Magnetic Resonance in Liquids*; Delft University: London, 1982.
(24) (a) Bax, A.; Freeman, R.; Morris, G. A. *J. Magn. Reson.* **1981**, *42*, 164. (b) Bax, A.; Freeman, R. *J. Magn. Reson.* **1981**, *44*, 542.
(25) Anteunis, M. J. O. *Bioorg. Chem.* **1977**, *6*, 1.
(26) Pretsch, E.; Seibl, J.; Simon, W.; Clerc, T. In *Tables of Spectral Data for Structure Determination of Organic Compounds*; Springer-Verlag: New York, 1983; p H255.
(27) Deber, C. M.; Pfeiffer, D. R. *Biochemistry* **1976**, *15*, 132.
(28) David, L.; Guittet, E.; Lallemand, J. Y.; Beloeil, J. C. *Nouv. J. Chim.* **1981**, *5*, 531.
(29) (a) Bodenhausen, G.; Freeman, R. *J. Magn. Reson.* **1977**, *28*, 303. (b) Freeman, R.; Morris, G. A. *J. Chem. Soc., Chem. Commun.* **1978**, 684.
(30) Seto, H.; Otake, N. *Heterocycles* **1982**, *17*, 555.

Table V. Stability Constants of the Alkali and Alkali-Earth Complexes Formed with X-14885A and Calcimycin (A-23187)[a]

alkali cations	log K_{AM} for $A^- + M^+ \rightleftarrows AM$		alkali-earth cations	log K_{AM^+} for $A^- + M^{2+} \rightleftarrows AM^+$		log K_{A_2M} for $AM^+ + A^- \rightleftarrows A_2M$	
	X-14885A	A-23187		X-14885A	A-23187	X-14885A	A-23187
Li^+	4.1	4.1[b]	Mg^{2+}	7.1	7.6[b]	7.3	8.3[b]
Na^+	3.7	3.4[b]	$I = 0.1$	5.2	6.2 ± 0.2[d]	7.0 ± 0.2	7.6 ± 0.3[d]
	3.7[c]		Ca^{2+}	7.9	8.2[b]	8.0	8.0[b]
K^+	3.0	2.4[b]	$I = 0.1$	6.0	6.4 ± 0.2[d]	7.8 ± 0.2	7.8 ± 0.2[d]
	3.0[c]		Sr^{2+}	6.8	6.7[b]	6.9	7.5[b]
Rb^+	2.7	2.0[b]	Ba^{2+}	5.8	6.2[b]	6.2	6.2[b]
	2.8[c]						

[a] Solvent, methanol; $I = 0$; $T = (25.0 \pm 0.1)$ °C. [b] From ref 9a. [c] Assuming the formation of both AMH^+ and AM (log $K_{ANaH^+} = 1.5$; log $K_{AKH^+} = 1.2$; log $K_{ARbH^+} = 1.5$). [d] From ref 11.

metric and spectrophotometric measurements) for the antibiotic X-14885A in methanol. For calcimycin, a pK_2 value of 3.1 was obtained and assigned to the protonation of the secondary amine substituent on the benzoxazole moiety. One could envisage, in the case of X-14885A, the protonation of the oxazolic nitrogen, which does occur circa $-\log [H^+] = 2$ in methanol.

Protonation constants (Table IV) and their corresponding absorption spectra (Figure 3) were calculated with the program LETAGROP-SPEFO.[19] As for calcimycin,[9,11] the spectra of the protolytic species of the ionophore X-14885A appear as a combination of two bands related to the transitions of the ketopyrrole moiety (located at about 250–260 and 290 nm) and of the three bands[31-34] related to the benzoxazole moiety (located here at about 205–210, 250–260, and 320 nm). Compared to calcimycin, the last band for the benzoxazole moiety is strongly shifted (40 to 60 nm) to shorter wavelengths and appears in compound X-14885A as a shoulder of the strong 290-nm ketopyrrole band.

(b) Alkali and Alkali-Earth Complexes with X-14885A in Methanol. From the previous studies concerning other ionophores of the same family, the existence of unprotonated and of protonated complexes could be postulated a priori. The formation of the second species occurs in acid conditions. Although the formation of the neutral species AM always predominates, the formation of AMH^+ is possible in methanol when M^+ is an alkali-metal cation. This was clearly observed with monensin, grisorixin, nigericin, and alborixin;[35] the experiments were unconclusive in the case of lasalocid.[36] For the experiments conducted using two indicative glass electrodes, it was possible to proceed with the calculations assuming either the formation of the two complexes AMH^+ and AM or the formation of AM only. Data thus obtained are collected on Table V. The stability constants for the AMH^+ complexes are small, and ignoring them does not affect the determination of the stability constants of the AM species.

Although the slight protonation of the oxazolic nitrogen reduces the accuracy of the potentiometric data treatment in acid media, it appears that no significant amount of species AHM^{2+} or $(AH)_2M^{2+}$ was formed when M^{2+} is an alkaline-earth cation. A good agreement with the experimental results was obtained in all cases, assuming, as previously for calcimycin, the formation of the successive complexes AM^+ and A_2M in methanol. Our calculated stability constants are given in Table V, along with the values previously reported for calcimycin.[9a]

Liu et al.[15] studied displacement of $^{45}Ca^{2+}$ from its X-14885A complex by other alkaline-earth cations in toluene/1-butanol (70:30) in equilibrium with an aqueous phase. The binding sequence of the ionophore was found to be $Mg^{2+} > Ca^{2+} > Sr^{2+} > Ba^{2+}$. These results are not in agreement with ours for Mg^{2+} and Ca^{2+}. We found that the complexation of Ca^{2+} by X-14885, like calcimycin, is stronger than the complexation of Mg^{2+}. Moreover, our determination of the equilibrium constant for extraction[13] of Ca^{2+} and Mg^{2+} by X-14885A has shown that calcium is more strongly complexed than magnesium.

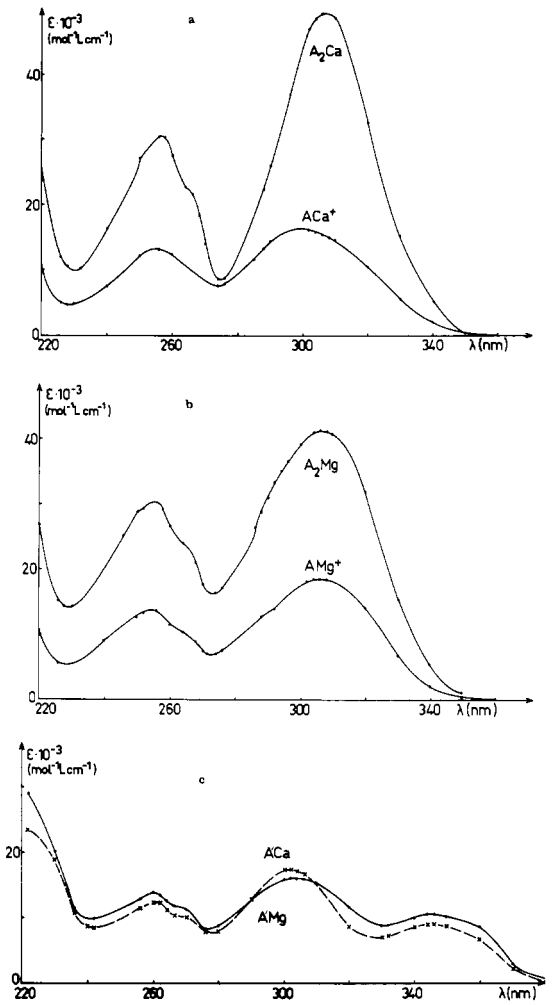

Figure 4. Electronic spectra of the complexes A_2M, AM^+, and A'M formed with the ionophore X-14885A in methanol: (a) calcium complexes A_2Ca and ACa^+; (b) magnesium complexes A_2Mg and AMg^+; (c) calcium and magnesium complexes A'Ca and A'Mg.

The magnesium and calcium X-14885A complexes, which have appeared under strongly basic conditions, (Figure 2b), have been suggested by the numerical treatment[19] of the potentiometric and spectrophotometric data to be 1:1 2-fold deprotonated ionophore/cation neutral complexes, A'M assuming

$$A^- \rightleftarrows A'^{2-} + H^+ \quad (1a)$$

$$A^- + M^{2+} \overset{\beta_{A'M}}{\rightleftarrows} A'M + H^+ \quad (1b)$$

(31) Jones, R. A. In *Advances in Heterocyclic Chemistry*; Katritzky, A. R.; Boulton, A. J., Eds.; Academic Press: New York, 1970; Vol. XI, p 459.
(32) Passerini, R. *J. Chem. Soc.* **1954**, *11*, 2256.
(33) Mason, S. F. In *Physical Methods in Heterocyclic Chemistry*, Katritzky, A. R., Ed.; Academic Press: New York, 1963; Vol. II, p 59.
(34) Rao, C. N. R. *Ultraviolet and Visible Spectroscopy*, 2nd ed.; Butterworths: London, 1967.
(35) Juillard, J.; Pointud, Y.; Tissier, C.; Jeminet, G. In *Physical Chemistry of Transmembrane Ion Motions*; Spach, G., Ed.; Elsevier: Amsterdam, The Netherlands, 1983; p 239–246.
(36) Pointud, Y.; Juillard, J. *J. Chem. Soc., Faraday Trans. 1* **1988**, *84*, 959.
(37) Diebler, H.; Eigen, M.; Ilgenfritz, G.; Maass, G.; Winkler, R. *Pure Appl. Chem.* **1969**, *20*, 93.

and the logarithm of the thermodynamic constant values were calculated to be equal to -5.48 ± 0.05 for A'Ca and -5.85 ± 0.06 for A'Mg. Our potentiometric and spectrophotometric measurements do not allow us to distinguish between a neutral methoxylated complex AMOMe or a neutral deprotonated A'M complex. It is known from previous work[10] that AMOMe complexes with calcimycin show very little change in the benzoxazole absorption (370 nm), the α-ketopyrrole absorption being more affected by the methoxylation of the AM^+ complexes. In our case, the similarity of the thermodynamic constants for calcium and magnesium complexes and the large change in the absorption of the benzoxazole moiety (Figure 4c) seem to favor the deprotonation of the -OH group of X-14885A.

Electronic spectra corresponding to the various species involved have been calculated from the spectrophotometric data on Ca^{2+} and Mg^{2+} X-14885A interactions in methanol ($I = 0.1$; Figure 4). The electronic spectra corresponding to AM^+ and A_2M species possess similar λ_{max} although the intensity of the last one is about twice that of the first. This suggests that, in the A_2Ca and A_2Mg complexes, the two ionophore anions play a similar role. There is a bathochromic shift (about 15 nm) as well as an hyperchromic effect on the 290-nm band, which shows that the ketopyrrole moiety is directly involved as a ligand. As a consequence of the shift of this ketopyrrole band, the 320-nm band of the benzoxazole moiety is masked in the resulting spectrum, markedly widening the peak from 280 to 350 nm.

(3) Calcium and Magnesium Complexation Mechanism. Kinetic Measurements. Formation and dissociation kinetics of the calcium and magnesium complexes formed with the ionophore X-14885A were studied in methanol. We have also studied the formation kinetics of the calcium and magnesium complexes of the ionophore A-23187 in order to achieve the comparison between both ionophores using experimental data. Calculated values were available[11] for the formation kinetics of A-23187 complexes.

(a) Formation Kinetics of the Calcium and Magnesium Complexes with X-14885A and A-23187 in Methanol. We have studied the formation kinetics of the neutral A_2M magnesium and calcium complexes with both the natural ionophores X-14885A and A-23187 at various proton concentrations. Because the reactions became too fast for the stopped-flow technique, we were unable to adopt pseudo-first-order conditions (with large excess of free ionophore or of cations).

In order to reduce the rate of reaction, a 2:1 ionophore/cation concentration ratio was chosen. With the help of the thermodynamic data (Tables IV and V) and of the program HALTAFALL,[21] we calculated the formation curves of A_2M species as a function of hydrogen ion concentrations (Figure 5 for A_2Mg with X-14885A and A-23187). The A_2M complexes are formed in a large range of $-\log [H^+]$, when the ionophore concentration is twice that of the cation-concentration. The spectrophotometric kinetic data are consistent (for both ionophores with calcium and magnesium) with the relationship in eq 2 where D_0, D, and D_∞ are,

$$\frac{D - D_0}{D_\infty - D} \approx 2[M^{2+}]_0 k_{obs} t \qquad (2)$$

respectively, the initial, the instantaneous, and the final optical density and $[M^{2+}]_0$ is the initial metal concentration. Equation 2 is related to the classical second-order rate law

$$v = \frac{d[A_2M]}{dt} = k_{obs}[M^{2+}][A]_{total} \qquad (3)$$

where k_{obs} is the experimental second-order rate constant and $[A]_{total}$ is the total instantaneous concentration of free ionophore. It was verified that the rate law (eq 3) was independent of the wavelength chosen for observation and of the initial concentrations of the reactants, the ratio 2:1 ionophores/cation being fixed. The values of k_{obs} determined at various concentrations of protons for the formation of A_2Ca and A_2Mg with A-23187 and X-14885A are presented in parts a and b of Table VI, respectively. For the range of proton concentrations covered, calculations show that the fraction of the ionophore protonated changed significantly, except for Ca^{2+} with X-14885A.

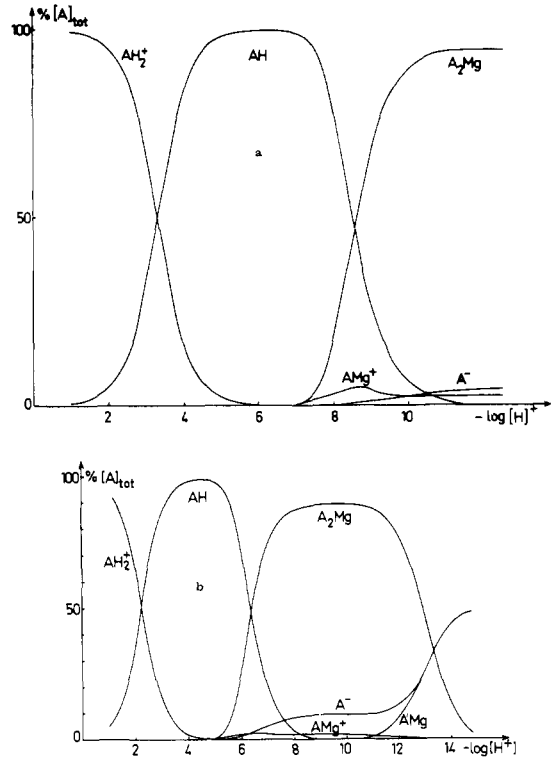

Figure 5. Formation curves as a function of hydrogen ion concentrations for the A_2M complexes with A-23187 and X-14885A: (a) [A-23187] = 2.0×10^{-5} mol L^{-1}, $[Mg^{2+}] = 1.0 \times 10^{-5}$ mol L^{-1}; (b) [X-14885A] = 2.7×10^{-5} mol L^{-1}, $[Mg^{2+}] = 1.35 \times 10^{-5}$ mol L^{-1}. Solvent, methanol; $I = 0.1$; $T = 25.0 \pm 0.1$ °C.

The values of k_{obs} as a function of $-\log [H^+]$ are presented in Figure 6 for the formation of A_2Mg with the both ionophores considered. The sigmoidal form of the curves obtained suggests two competing reactions via the anionic species A^- of the free ionophores and via the protonated ones, AH. It was observed that, over the range of proton concentrations covered by the kinetic experiments, the antibiotics protonation equilibria significantly shifted, except for A_2Ca with X-14885A (Table VI). Furthermore, the one-step mechanism observed and the rate law (eq 3) found to be well verified suggest that the rate-limiting step in the complexation mechanism is associated with the formation of the AM^+ complex. The corresponding mechanism (eq 4) is proposed and

$$\begin{array}{l} 2A^- + M^{2+} \xrightarrow{k_1} AM^+ + A^- \xrightarrow{\text{fast}} A_2M \\ + \\ 2H^+ \\ K_1 \updownarrow \\ 2AH + M^{2+} \xrightarrow{k_2} AM^+ + AH + H^+ \xrightarrow{\text{fast}} A_2M + 2H^+ \end{array} \qquad (4)$$

leads to the following form of the rate law (eq 3):

$$v = \frac{d[A_2M]}{dt} = k_{obs}[M^{2+}][A]_{total} = [M^{2+}]\{k_1[A^-] + k_2[AH]\} \qquad (5)$$

The experimental values (Table VI) of k_{obs} have been fitted to the mathematical expression (eq 6) calculated from the proposed relation (eq 5). The values of the rate constants k_1 and k_2 and

$$k_{obs} = \frac{k_1 + k_2 K_1[H^+]}{1 + K_1[H^+]} \qquad (6)$$

of the thermodynamic constant K_1 have been determined from the observed rate constants. This determination was performed in two steps:

(1) At low hydrogen ion concentrations, $K_1[H^+]$ being small and assuming that $k_1 \gg k_2$, the following expression is obtained:

$$1/k_{obs} = 1/k_1 + K_1[H^+]/k_1 \qquad (7)$$

Table VI. Experimental Second-Order Rate Constants for the Formation of the Magnesium and Calcium A_2M Complexes as a Function of $[H^+]$[a]

	$A^- + H^+ \rightleftarrows AH$			
$[H^+]$, mol L^{-1}	$\frac{[A^-]}{[A]_{total}}$, %	$\frac{[AH]}{[A]_{total}}$, %	Ca^{2+}, $k_{obs} \times 10^{-6}$, mol^{-1} L s^{-1}	Mg^{2+}, $k_{obs} \times 10^{-5}$, mol^{-1} L s^{-1}
		A. With A-23187		
6.1×10^{-12}	87.8	12.2		39.3 ± 3.4
1.3×10^{-11}	76.7	23.3		37.4 ± 3.2
1.5×10^{-11}				
3.1×10^{-11}	58.9	41.4	101 ± 18	30.4 ± 2.4
3.8×10^{-11}			95 ± 14	
7.5×10^{-11}	36.9	63.1	74 ± 9	
8.8×10^{-11}	33.3	66.7		17.9 ± 1.1
1.3×10^{-10}	24.9	75.1	52 ± 8	
2.1×10^{-10}	17.1	82.9		9.4 ± 0.5
2.2×10^{-10}	16.5	83.5	39 ± 5	
1.5×10^{-9}	2.8	97.2	5.8 ± 0.3	6.3 ± 0.3
2.2×10^{-9}	1.9	98.1	3.6 ± 0.2	
3.0×10^{-9}	1.4	98.6		3.6 ± 0.2
4.0×10^{-9}	1.1	98.9	2.3 ± 0.2	
6.4×10^{-9}	0.7	99.3	1.6 ± 0.1	
7.1×10^{-9}	0.6	99.4		1.9 ± 0.1
8.8×10^{-9}	0.5	99.5	1.6 ± 0.2	
1.2×10^{-8}	0.4	99.6	1.7 ± 0.1	
1.4×10^{-8}	0.3	99.7		1.0 ± 0.1
1.7×10^{-8}	0.2	99.8		0.9 ± 0.1
2.3×10^{-8}	0.2	99.8	1.4 ± 0.1	
2.5×10^{-8}	0.2	99.8		1.0 ± 0.1
		B. With X-14885A		
1.3×10^{-9}	95.0	5.0		86 ± 6
3.2×10^{-9}	88.0	12.0		85 ± 2
7.9×10^{-9}	75.7	34.3		74 ± 5
3.2×10^{-8}	45.0	55.0		54 ± 4
2.5×10^{-7}	9.0	91.0	95 ± 12	8.4 ± 0.5
6.0×10^{-7}	3.8	96.2	43 ± 4	
9.1×10^{-7}	2.5	97.5	29 ± 2	
1.2×10^{-6}	2.0	98.0		4.4 ± 0.4
2.0×10^{-6}	1.5	98.5	14 ± 2	
2.5×10^{-6}	0.9	99.0		2.2 ± 0.3
3.1×10^{-6}	0.6	99.3	9 ± 1	
4.5×10^{-6}	0.4	99.6	7 ± 1	
7.9×10^{-6}	0.3	99.7		2.0 ± 0.3

[a] Solvent, methanol; $I = 0.1$; $T = (25.0 \pm 0.1)$ °C. The uncertainties were calculated with 2σ.

(2) At high hydrogen ion concentrations, the value of $K_1[H^+] \gg 1$ and the form of the observed rate constant becomes

$$k_{obs} = k_2 + (k_1/K_1)(1/[H^+]) \quad (8)$$

In the former step, a linearization of $1/k_{obs}$ versus $[H^+]$ leads to the values of k_1 and K_1, and, in the latter step, a linearization of k_{obs} versus $1/[H^+]$ leads to the value of k_2 and enables a check of the ratio k_1/K_1. A linear least-squares method was used, and the calculated values are reported in Table VII.

Note the excellent agreement between the values of the thermodynamic protonation constants obtained by equilibrium studies (Table IV) and that calculated with this mechanism from kinetic measurements (Table VII). Formation of A_2M is significantly faster for X-14885A than for calcimycin; this is especially true for the calcium complex. Like A-23187, X-14885A binds calcium faster than magnesium via the monoprotonated or the deprotonated ionophore. A decrease of more than 1 order of magnitude in the formation rate constants is induced by the protonation of the carboxylic acid for the both ionophores. Because the reactions were too fast, the k_1 relative to the calcium binding by A^- could not be precisely determined.

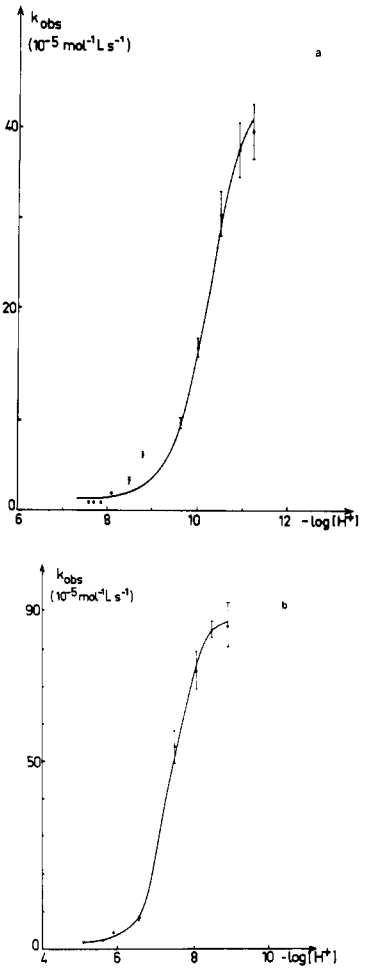

Figure 6. Variation of the experimental second-order rate constants for the formation of the complex A_2Mg as a function of $-\log [H^+]$: (a) with A-23187; (b) with X-14885A. Solvent, methanol; $I = 0.1$; $T = 25.0 \pm 0.1$ °C.

(b) Dissociation Kinetics of the Calcium and Magnesium Complexes of X-14885A in Methanol. The dissociation kinetics of the alkaline-earth cation complexes was studied in absolute methanol. The overall reactions for the dissociation of both complexes AM^+ and A_2M may be written as follows:

$$AM^+ + H^+ \rightarrow AH + M^{2+} \quad (9)$$

$$A_2M + 2H^+ \rightarrow 2AH + M^{2+} \quad (10)$$

Note that the ionophore liberated by these reactions is very rapidly equilibrated with the hydrogen ion in the medium. Thus, at higher hydrogen ion concentrations, the biprotonated AH_2^+ form of the antibiotic will be present.

The dissociation of these complexes was followed using the stopped-flow spectrophotometer set at 310 nm; the various concentrations of hydrogen ion employed as reactants of the reaction

Table VII. Kinetic and Thermodynamic Parameters Determined for the Formation of the Calcium and Magnesium A_2M Complexes with the Ionophores X-14885A and A-23187[a]

antibiotics	cations	$k_1 \pm \sigma$, mol^{-1} L s^{-1}	$k_2 \pm \sigma$, mol^{-1} L s^{-1}	$pK_1 \pm \sigma$
X-14885A	Ca^{2+}	$>10^8$	$(1.2 \pm 0.4) \times 10^6$	
	Mg^{2+}	$(1.1 \pm 0.2) \times 10^7$	$(1.8 \pm 0.4) \times 10^5$	7.8 ± 0.1
A-23187	Ca^{2+}	$>5 \times 10^7$	$(6 \pm 1) \times 10^5$	
	Mg^{2+}	$(4.6 \pm 0.1) \times 10^6$	$(1.2 \pm 0.4) \times 10^5$	10.26 ± 0.04

[a] Solvent, methanol; $I = 0.1$; $T = (25.0 \pm 0.1)$ °C.

Table VIII. Values of the Observed First-Order Rate Constants as a Function of Hydrogen Ion Concentrations for the Decomplexation of Calcium and Magnesium X-14885A Complexes[a]

$[H^+]$, mol L^{-1}	k_{obs} (s^{-1}) for $A_2Ca + 2H^+ \rightarrow 2AH + Ca^{2+}$	k_{obs} (s^{-1}) for $A_2Mg + 2H^+ \rightarrow 2AH + Mg^{2+}$
2.5×10^{-5}	13.2 ± 0.1	2.15 ± 0.04
3.1×10^{-5}	18.8 ± 0.2	2.32 ± 0.04
6.2×10^{-5}		2.86 ± 0.04
8.8×10^{-5}	23.6 ± 0.3	1.61 ± 0.01
9.9×10^{-5}	23.4 ± 0.4	
1.36×10^{-4}		2.7 ± 0.1
1.55×10^{-4}	43.4 ± 0.9	3.19 ± 0.04
1.73×10^{-4}	59 ± 1	3.29 ± 0.06
2.06×10^{-4}	65.6 ± 0.6	3.38 ± 0.06
2.12×10^{-4}	50 ± 1	
2.14×10^{-4}	52 ± 1	
2.49×10^{-4}	76 ± 1	4.03 ± 0.06
2.69×10^{-4}	68 ± 2	5.0 ± 0.1
2.90×10^{-4}	85 ± 2	5.11 ± 0.09
3.16×10^{-4}	91 ± 2	5.68 ± 0.07
3.26×10^{-4}	103 ± 2	
3.29×10^{-4}	103 ± 1	
3.32×10^{-4}		5.0 ± 0.1
4.11×10^{-4}	118 ± 3	7.6 ± 0.2
4.34×10^{-4}		7.9 ± 0.2
4.50×10^{-4}	124 ± 4	8.8 ± 0.3
4.65×10^{-4}	133 ± 3	7.7 ± 0.1
5.20×10^{-4}	143 ± 3	7.6 ± 0.1
5.54×10^{-4}	137 ± 5	9.3 ± 0.2
5.61×10^{-4}		8.7 ± 0.3
6.68×10^{-4}	194 ± 6	13.4 ± 0.3
7.32×10^{-4}		8.2 ± 0.2
7.52×10^{-4}	204 ± 5	11.5 ± 0.1
7.80×10^{-4}	200 ± 7	19.9 ± 0.4
8.89×10^{-4}	233 ± 8	16.3 ± 0.5
1.119×10^{-3}		17.6 ± 0.5
1.477×10^{-3}		22.5 ± 0.5
1.789×10^{-3}		29 ± 1
2.260×10^{-3}		32 ± 1
2.485×10^{-3}		28.6 ± 0.6
3.615×10^{-3}		55 ± 2
3.927×10^{-3}		47.1 ± 0.6
4.518×10^{-3}		65 ± 2
5.369×10^{-3}		57.3 ± 0.8
5.540×10^{-3}		72 ± 2
6.798×10^{-3}		77 ± 1
6.824×10^{-3}		79 ± 2
1.0428×10^{-2}		120 ± 2

[a] Solvent, methanol; $I = 0.1$; $T = (25.0 \pm 0.1)$ °C. The uncertainties were calculated with 2σ.

10 were constant during the dissociation (concentrations in excess or buffered solutions). The values of the experimental first-order rate constants, k_{obs}, determined in this way are given in Table VIII for calcium and magnesium A_2M complexes. The variation of k_{obs} with the hydrogen ion concentrations is linear for both A_2Ca and A_2Mg in the $[H^+]$ range studied (Figure 7a). Figure 7a shows clearly that the complex A_2Ca dissociates more rapidly than the corresponding A_2Mg complex. The variations of the observed first-order rate constants as a function of $[H^+]$ do not tend toward an asymptotic value at high hydrogen ion concentrations, as was the case for calcimycin (Figure 7b). The ionophore X-14885A does not form any intermediate protonated complex in the acid dissociation pathway of its A_2M magnesium and calcium complexes.

In order to propose a dissociation mechanism, it was necessary to investigate the influence of the presence of charged AM^+ complexes on the kinetic data. Due to solubility considerations, it was not possible to prepare pure AM^+ solutions with a large excess of cation. We have prepared AM^+ solutions up to 90% AM^+ and 9% A_2M complexes (Table IX) and measured the values of the first-order rate constants obtained in these conditions. The k_{obs} values obtained at the same $[H^+]$ are identical, within experimental error, for the dissociation of the dimeric A_2Mg complex and the monomeric AMg^+ complex formed with the ionophore

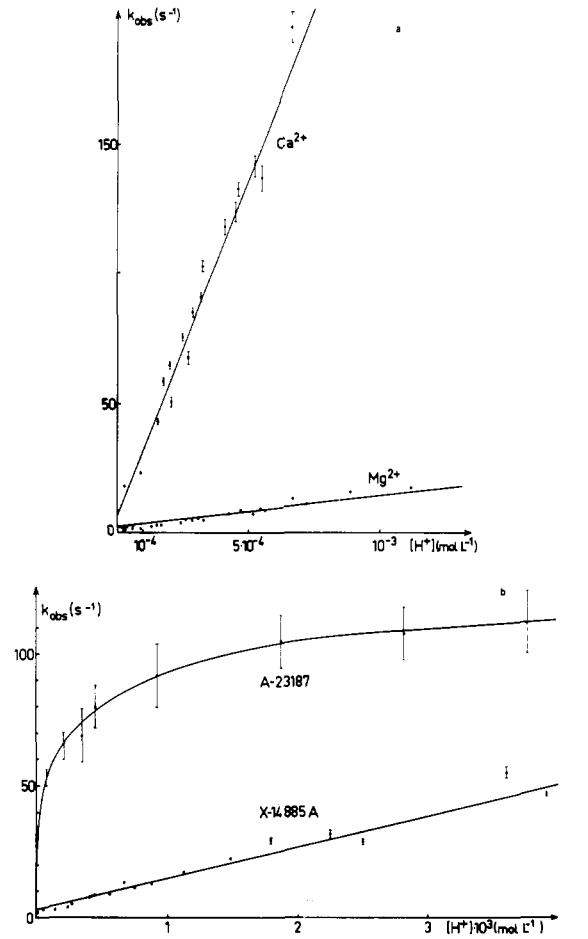

Figure 7. Variation of the observed first-order rate constants as a function of $[H^+]$: (a) for the dissociation of the A_2M magnesium and calcium complexes with X-14885A; (b) for the dissociation of the A_2Mg complexes with A-23187[11] and X-14885A, respectively. Solvent, methanol; $I = 0.1$; $T = 25.0 \pm 0.1$ °C.

Table IX. Influence of Various Concentrations of A_2Mg and AMg^+ Complexes Formed with the Ionophore X-14885A on the Dissociation Kinetic Data[a]

$[H^+]$, mol L^{-1}	k_{obs},[b] s^{-1}	k_{obs},[c] s^{-1}	k_{obs},[d] s^{-1}
7.3×10^{-4}	8.2 ± 0.2		13 ± 2
1.48×10^{-3}	22.5 ± 0.5		22 ± 5
2.27×10^{-3}	32 ± 1	29 ± 2	30 ± 4
2.97×10^{-3}	36 ± 1	34 ± 2	
3.60×10^{-3}	46 ± 1	40 ± 3	
4.46×10^{-3}	57 ± 1	56 ± 3	

[a] Solvent, methanol; $I = 0.1$; $T = (25.0 \pm 0.1)$ °C. The uncertainties were calculated with 2σ. [b] $[A_2Mg]_0/[A]_{total} = 0.93$, $[AMg^+]_0/[A]_{total} = 0.02$. [c] $[A_2Mg]_0/[A]_{total} = 0.47$, $[AMg^+]_0/[A]_{total} = 0.52$. [d] $[A_2Mg]_0/[A]_{total} = 0.09$, $[AMg^+]_0/[A]_{total} = 0.90$.

X-14885A in methanol. This indicates that the dissociation of the AMg^+ and A_2Mg complexes have the same rate-limiting step and that this step is associated with the dissociation of the AMg^+ complex. The loss of the first ionophore molecule ($A_2M \rightarrow AM^+ + A^-$) is fast in acidic media. The proposed mechanism for the dissociation of the alkali-earth cation complexes of the ionophore X-14885A (eq 11) is written below and compared to that of A-23187 (eq 12). The direct decomplexation pathway occurs in the absence of hydrogen ions and is related to the thermodynamic stability of the AM^+ complexes (Table V). We have calculated the k_D and k'_H values for X-14885A (mechanism 11) and presented the corresponding values[11] for the dissociation of the A_2M and AM^+ complexes formed with calcimycin (Table X). We note that the lability of the AM^+ complexes is significantly higher for the calcium and magnesium complexes of X-14885A than those of A-23187. The rate constants for proton catalysis

X-14885A

$$A_2M + 2H^+ \xrightarrow[\text{fast}]{K'_{A_2M}} AM^+ + AH + H^+ \xrightarrow{k'_H} 2AH + M^{2+} \quad (11)$$

hydrogen ion assisted decomplexation

$$AM^+ \xrightarrow{k_D} A^- + M^{2+}$$

direct decomplexation

A-23187

$$A_2M + 2H^+ \xrightarrow[\text{fast}]{K'_{A_2M}} AM^+ + AH + H^+ \xrightarrow{K_{AMH^{2+}}} AMH^{2+} + AH \xrightarrow{k_H} 2AH + M^{2+} \quad (12)$$

hydrogen ion assisted decomplexation

$$AM^+ \xrightarrow{k_D} A^- + M^{2+}$$

direct decomplexation

is 2 or 3 orders of magnitude lower in the X-14885A complexes than in the calcimycin ones.

Discussion

Free Ionophore X-14885A. Very few structural data are available except the X-ray structure of the X-14885A sodium salt.[15b] In order to understand the physicochemical behavior of this new ionophore and to compare it to that of calcimycin, we have carried out an NMR study of the free ionophore in CD_3OD and in $CDCl_3$. The X-14885A structure can be considered as constituted of three distinctive parts: a spiroketal backbone and two different arms, namely, the benzoxazole and the ketopyrrole moieties (Figure 8). Free rotations are allowed in the "hinge regions", about C_8–C_9, C_9–C_{10}, C_{18}–C_{19}, and C_{19}–C_{20} bonds. Analysis of the coupling constants and chemical shifts for the ^1H and ^{13}C resonances allows us to propose preferential conformations. Comparison with calcimycin using results obtained by us in CD_3OD and by others in $CDCl_3$[25,27] is then possible.

NMR spectra of the free antibiotic X-14885A in $CDCl_3$ have shown that, for *the tetrahydropyran substituted by the ketopyrrole*, the following values of the coupling constants were obtained: $J_{17,18}$ = 2.0 Hz, $J_{16A,17}$ = 5.0 Hz, $J_{16B,17}$ = 2.0 Hz, and $J_{15A,16A}$ = 13.5 Hz. These values suggest a classical chair conformation, with H_{18}, $Me_{17'}$, H_{16A}, and H_{15A} in axial positions and C_{18}–C_{19} in equatorial positions. The small $J_{17,18}$ value corresponds to an axial–equatorial coupling in the presence of an oxygen antiperiplanar to H_{17}.[38] The low δ ^{13}C chemical shift for $Me_{17'}$ (10.6 ppm) is in agreement with its axial position.

The second tetrahydropyran ring shows similar features; the C_9–C_{10} bond and $Me_{11'}$ are, respectively, in equatorial and axial positions, thus in cis configuration to each other. The spiroketal backbone then constitutes a rigid part in the molecule, with an axial–axial geometry on the C_{14} junction, as observed in the solid state for the X-14885A sodium salt[15b] (Figure 8).

The position of the *benzoxazole* ring is determined by the rotators 8–9 and 9–10. Considering the coupling constant values for $J_{10,9(pro\text{-}S)}$ = 9.0 Hz and $J_{10,9(pro\text{-}R)}$ = 6.0 Hz, one can assume a preferential conformation around the C_9–C_{10} bond, with dihedral angles of, respectively, 150° and 30° for $H_{9(pro\text{-}S)}$ and $H_{9(pro\text{-}R)}$ with H_{10} (Table XI; Figure 9a). The value of $^2J_{(9)}$ = 15.0 Hz is in favor of a definite spatial position of the CH_2-9 methylenic protons with respect to the plane of the benzoxazole ring, with $H_{9(pro\text{-}R)}$ eclipsing the adjacent bond of the oxazole.[39] Free rotation around the C_8–C_9 bond would result in $^2J_{(9)}$ = 14 Hz.[25,39]

For the *ketopyrrole* arm, the antiperiplanar relationship between H_{18} and H_{19} is clearly shown by a coupling constant of 10.0 Hz (Table XI). Unfortunately, rotator 19–20 cannot be investigated by this approach. If we consider the preferential conformations proposed for the other potentially free-rotating bonds and the rigid character of the spiroketal backbone, together with a deshielding

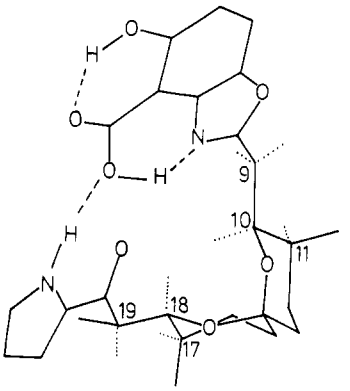

Figure 8. Postulated cyclic conformation of X-14885A, acid form AH in $CDCl_3$.

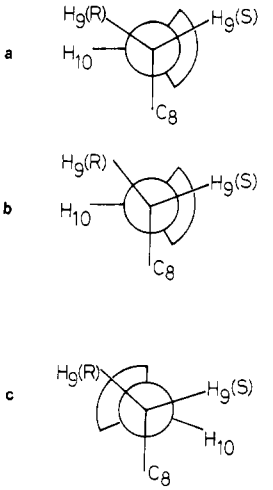

Figure 9. Postulated preferential orientations of the substituents on the C_9–C_{10} bond of X-14885A: (a) acid form AH in $CDCl_3$; (b) acid form AH in CD_3OD; (c) postulated preferential orientations of the substituents on the C_9–C_{10} bond of X-14885A in the A_2Mg complex in $CDCl_3$.

effect observed for the pyrrole NH (δ_{NH} = 9.62 ppm), it seems very likely that the X-14885A molecule, in the acid form, adopts a cyclic conformation in $CDCl_3$ with a head-to-tail hydrogen bonding between the carboxylic group and the –NH (Figure 8), as observed in the solid state for calcimycin.[2b]

NMR data obtained for the free antibiotic X-14885A in CD_3OD are given in Tables I and III. The main significant variations registered on comparison with $CDCl_3$ are located in the C_8–C_9–C_{10} region. Values for the dihedral angles increase from 150° to 170° and 30° to 50°, respectively, for $H_{9(pro\text{-}S)}$–H_{10} and $H_{9(pro\text{-}R)}$–H_{10} (Table XI; (Figure 9b). Further, the J_{gem} value for H_9 methylenic protons is 14 Hz, which could correspond to a rotation of the benzoxazole system around the C_8–C_9 bond and/or an increasing mobility of the aromatic group.[39a] This conformational change is corroborated by the small shielding effect observed for protons H_{10} and H_{18}. In this solvent the head-to-tail hydrogen bonding (Figure 8) cannot be inferred. The same results have been obtained for calcimycin in CD_3OD, in agreement with recent observations made on CD spectra of this ionophore.[39b]

It can be concluded from these data that the solution conformations of the ionophores calcimycin and X-14885A are very similar either in $CDCl_3$ or in CD_3OD.

The UV absorption band of calcimycin at 350–380 nm is due solely to the benzoxazole moiety and extremely sensitive to any change in substituents. No absorbance appears in this region for X-14885A unlike A-23187, which shows absorption peaks for the anionic form at 350 nm and for its protonated species at 380 nm.[11] The replacement of the secondary amine group in calcimycin by the hydroxide group in X-14885A makes a large shift (30 nm) toward shorter wavelengths. These absorption properties produce a widening in the characteristic peak of the ketopyrrole at 290

(38) Abraham, R. J.; Gatti, G. *J. Chem. Soc. B* **1969**, 961.
(39) (a) Barfield, M.; Grant, D. M. *J. Am. Chem. Soc.* **1963**, *85*, 1889. (b) Divakar, S.; Easwaran, K. R. K. *Biophys. Chem.* **1987**, *27*, 139.

Table X. Kinetic Parameters for the Dissociation of Calcium and Magnesium Complexes Formed with Calcimycin (A-23187) and X-14885A[a]

alkaline-earth cations	A-23187		X-14885A	
	k_D, s^{-1}	$k_H \times K'_{AMH^{2+}}$, mol^{-1} L s^{-1}	k_D, s^{-1}	k'_H, mol^{-1} L s^{-1}
Ca^{2+}	2 ± 1	(1.1 ± 0.6) × 10^8	7 ± 3	(2.6 ± 0.1) × 10^5
Mg^{2+}	0.3 ± 0.2	(3.3 ± 0.7) × 10^6	3.0 ± 0.8	(1.15 ± 0.03) × 10^4

[a] Solvent, methanol; I = 0.1; T = (25.0 ± 0.1) °C. The data concerning A-23187 came from ref 11.

Table XI. Coupling Constants and Dihedral Angles in the Hinge Regions of the Free Ionophores X-14885A and A-23187 (Calcimycin) and of Their Neutral Magnesium Complexes[a]

protons	free ionophore X-14885A		X-14885A neutral A_2Mg complex in $CDCl_3$	free ionophore A-23187		A-23187 neutral A_2Mg complex in $CDCl_3$[25]
	in $CDCl_3$	in CD_3OD		in $CDCl_3$[25,27]	in CD_3OD	
10–9(pro-*S*)	9.0 [155]	11.0 [170]	3.25 [55]	7.3 [150]	10.0 [160]	2.3 [60]
10–9 (pro-*R*)	6.0 [35]	4.0 [50]	11.25 [175]	7.5 [30]	4.0 [40]	11.9 [180]
10–11	2.0 [90]	2.0 [90]	2.0 [90]	2.1 [90]	2.0 [90]	2.0 [90]
18–17	2.0 [90]	2.0 [90]	1.5 [90]	1.7 [90]	2.0 [90]	2.1 [90]
19–18	10.0 [180]	10.0 [180]	10.0 [180]	10.3 [180]	10.0 [180]	9.8 [180]

[a] Dihedral angles (deg) are presented in brackets and were deduced from Karplus-type relationship H–C–C–H.

nm for X-14885A. Furthermore, shoulders appear between 320 and 330 nm upon protonation (Figure 3). Like the protonation of the carboxylic group (AH), the second protonation of X-14885A significantly affects the benzoxazole absorption and very slightly the ketopyrrole absorption. In agreement with its low pK value (Table IV), the second protonation (AH_2^+) of the ionophore X-14885A could be attributed to the protonation of the oxazolic nitrogen.

The most striking result of the thermodynamic data is the decrease of more than 2 orders of magnitude of the pK value relative to the protonation of the carboxyl function in pure methanol, when X-14885A is compared to calcimycin. This property favors the existence of the anionic form A^- of the ionophore X-14885A in a large range of hydrogen ion concentrations. If we consider that the corresponding pK value of calcimycin decreases of about 3 orders of magnitude[11] from methanol to a mixed solvent, methanol/water (70:30 by weight), which can be accepted as a good model of membrane interface for valinomycin[40] and for calcimycin,[8,41,42] we can conclude that the anionic species A^- of X-14885A will be enormously favored at the interface lipidic membrane/water in biological systems. Conversely, the neutral species, which is the proton carrier in the membrane, is disfavored when X-14885A is compared to calcimycin.

Calcium and Magnesium X-14885A Complexes. In chloroform solution, the NMR spectrum of A_2Mg shows a symmetry for both the molecules of ionophore X-14885A. No broadened resonances were observed in ^1H and ^{13}C NMR spectra; thus, under our experimental conditions, ligand-exchange processes were not detected. For the proton spectra, resonances are normally shifted upfield in comparison with the free ligand, the highest effect (1.1 ppm) being noted for H_{18} followed by H-16_a (0.58 ppm) and H-17_e (0.50 ppm). This observation is in good agreement with a previous result reported on calcimycin magnesium salt by Anteunis,[25] who proposed a conformation in which the upfield shift of H_{18} was induced by the benzoxazole system. This was confirmed a few years later by the crystal structure of the complex, which contained a highly symmetrical octahedral coordination of the Mg^{2+} ion, the coordinating sites being the carboxylate oxygen, the ketopyrrole oxygen, and the oxazole nitrogen in each molecule;[43a] this dimeric structure was closely resembling that one described for the ferrous ion complexes.[43b]

We are thus led to think that X-14885A adopts a similar conformation in its dimeric association around the magnesium cation. In this interpretation, values for the coupling constants

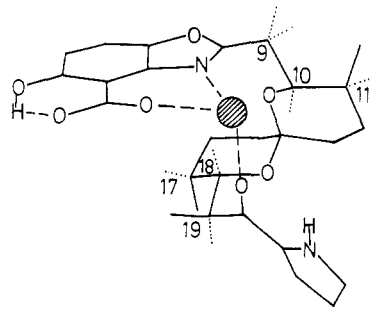

Figure 10. Representation of the association $X\text{-}14885A^-$, Mg^{2+} (half-structure).

of the C_9–C_{10} rotation are strongly affected, $^3J_{9(pro\text{-}R)\text{-}10}$ = 11.25 Hz and $^3J_{9(pro\text{-}S)\text{-}10}$ = 3.25 Hz. The $H_{9(pro\text{-}R)}$ proton stays almost antiperiplanar (175°) from an approximately clinal position (35°; Table XI) in the acid. The coupling constant $^2J_{(9)}$ is close to 13 Hz, which means that (Figure 9c) the adjacent bond of the oxazole almost bisects the H_{9R}–C_9–H_{9S} angle. The coupling constants in the spiroketal moiety are unaffected (Table III), as is the $^3J_{H_{18}\text{–}H_{19}}$ value. This part of the molecule is thus identical in the free ligand and in the complex. All the above information, together with the downfield effect observed in the ^{13}C spectrum for resonances C_2, C_8, C_{20}, C_{22}, and C_{24}, corroborate the features of the half-cavity, with the coordinating sites above (Figure 10).

As was the case for calcimycin,[25,27] the very low field position of the pyrrole NH proton (12.9 ppm) suggests an intermolecular hydrogen bond between this group and the carboxylate of the other unit in a dimeric association.

Like the free ionophore calcimycin and X-14885A, their A_2Mg complexes show very similar conformations in $CDCl_3$, according to previous NMR results[25,27,28] (Tables I–III). The replacement of the –NHMe by an –OH function on the benzoxazole ring and a methyl group missing in position 15 do not lead to important modifications in the overall conformation of the two microbial metabolites.

Further similarities have been observed in the thermodynamic data relative to the binding of either alkali or alkaline-earth cations by X-14885A and calcimycin (Table V). Stability constants of the complexes are roughly identical. But, X-14885A is more acidic than calcimycin by 2.5 pK units. Consequently, the formation of the complexes will be favored in a larger $[H^+]$ range and under acidic conditions. For these two ionophores, the stability constants of the alkali cations decrease, when the size of the cations increases (Table V). Such an effect is unusual in the family of the polyether carboxylic ionophores and restricted, to our knowledge, to the compounds akin to calcimycin. This could be rationalized by the small size of the cavity created by the head-to-tail hydrogen bond, which was observed in the crystalline state[15b] for the sodium complex of X-14885A. The stability of the 1:1 ionophore/cation

(40) Grell, E.; Funck, Th.; Eggers, F. In *Membranes*; Eisenman, G., Ed.; Marcel Dekker: New York, 1974; Vol. III, pp 148–157.
(41) Kaufman, R. F.; Taylor, R. W.; Pfeiffer, D. R. *Biochemistry* **1982**, *21*, 2426.
(42) Wulf, J.; Pohl, W. G. *Biochim. Biophys. Acta* **1977**, *465*, 471.
(43) (a) Alleaume, M.; Barrans, Y. *Can. J. Chem.* **1985**, *63*, 3482. (b) Baker, E.; Maslen, E. N.; Watson, K. J.; White, A. H. *J. Am. Chem. Soc.* **1984**, *106*, 2860.

Table XII. Kinetic and Thermodynamic Constants Relative to the AM^+ Complexes of X-14885A and A-23187

		kinetic measurements			
antibiotics	cations	formation k_1, mol^{-1} L s^{-1}	dissociation k_D, s^{-1}	equilibrium $\log \frac{k_1}{k_D}$	thermodynamic measurements: $\log K_{AM^+}$
X-14885A	Ca^{2+}	$>10^8$	7 ± 3		
	Mg^{2+}	$(1.1 \pm 0.2) \times 10^7$	3.0 ± 0.8	6.6 ± 0.3	5.2 ± 0.1
A-23187	Ca^{2+}	$>5 \times 10^7$	2 ± 1		
	Mg^{2+}	$(4.6 \pm 0.1) \times 10^6$	0.3 ± 0.2	7.2 ± 0.5	6.2 ± 0.1

complexes of X-14885A or calcimycin with the alkaline-earth cations is of about 3 orders of magnitude greater than the stability of the complexes with the alkali cations (Table V). This was also observed for the other ionophores with one exception (sodium monensin)[44] of the same family.

Comparing now the thermodynamic constants of the AM^+ complexes with calcimycin and X-14885A, AMg^+ is less than 1 order of magnitude lower for the latter of the two ionophores. This could be related to differences in the electronic distribution on the benzoxazole moiety due to a substituent effect of –OH compared to –NHMe. Such differences are sensitive to interactions with high charge density cations such as the proton, as illustrated by the protonation constants (Table IV), or the magnesium ion (Table V).

The most interesting property of the ionophores is their ability to form strong 2:1 ionophores/cation neutral complexes with divalent cations. For the calcium cation, the formation constant for the reaction $ACa^+ + A^- \rightleftarrows A_2Ca$ is equal to 10^8 mol^{-1} L in methanol for both X-14885A and calcimycin. For lasalocid[18] it is only 3×10^2 mol^{-1} L and 10^3 mol^{-1} L for X-14547A.[44] As shown in Table V, the successive A_2M stability constants are equal (even greater) to the AM^+ stability constants; they are markedly superior for Ca^{2+} and Mg^{2+} in the 0.1 mol L^{-1} solution of tetrabutylammonium perchlorate. Such a trend illustrates the great stability of the cavity formed by two anions of calcimycin or X-14885A, as indicated by the X-ray structure of A_2Mg with calcimycin.[43a]

Thermodynamically, calcimycin and X-14885A are effective ligands of alkaline-earth cations, especially for calcium and magnesium. X-14885A seems to be more selective for calcium compared to magnesium than calcimycin. The values of the stability constants in methanol are surprisingly large and do not correspond to an "optimal value" of 10^5 mol^{-1} L defined for an efficient uncharged carrier in this solvent.[45]

The complete complexation mechanism of calcium and magnesium has been provided by the kinetic study of formation and dissociation of A_2Mg and A_2Ca complexes formed with X-14885A and calcimycin in methanol. The rate-limiting steps of the formation and of the dissociation mechanisms of these complexes are associated with the charged complexes AM^+, the addition or the loss of the second ligand being faster. Several investigations have found evidence for the presence of the charged complex AM^+ at membrane interface for calcimycin.[3b,46,47] The important role of the charged complexes AM^+ at membrane interface in the cation transport through biological membranes have been definitely established. The acid–base conditions have drastic effects on either the formation kinetics or the dissociation kinetics of the complexes. Two formation pathways have been elucidated via the deprotonated ionophores A^- and via the monoprotonated species AH, the latter being at least 40 times slower than the former (Table VII). The difference in charge between A^- and AH cannot really explain this result. Diebler et al.[51,52] have shown that the intramolecular hydrogen bond between the hydroxyl and the carboxyl groups in salicylate ligands affect their rates of reaction with cations by 2 orders of magnitude.[52] In the case of X-14885A, the internal hydrogen bond between the nitrogen of the benzoxazole moiety and the hydrogen of the carboxylic group must also be broken for the complex formation. This could explain why the kinetic constant k_2 is of 3 orders of magnitude less than k_1 (Table VII). The dissociation mechanism of calcium and magnesium complexes with X-14885A and with calcimycin have shown a hydrogen ion assisted pathway. A protonated intermediate complex AMH^{2+} has appeared in the dissociation mechanism of the calcium and magnesium calcimycin complexes. If we compare the pK value of the secondary amine in the free calcimycin, which is equal to 3.3, to the values[11] of $\log K_{ACaH^{2+}} = 5.2$ and $\log K_{AMgH^{2+}} = 4.3$, the protonation site of the charged complexes is assigned to be the secondary amine on the benzoxazole moiety of calcimycin. This hypothesis is confirmed by the fact that ionophore X-14885A, for which an –OH group replaces the $-NHCH_3$ on the benzoxazole ring, does not show any intermediate protonated complexes in the dissociation mechanism of its magnesium and calcium complexes. A classical catalysis of the hydrogen ion on the dissociation of the complexes has been found for X-14885A, this catalysis being much less efficient by 2 or 3 orders of magnitude than the acid dissociation pathway of calcimycin (Table X). This result could be easily explained by an intramolecular protonation of the carboxylic function by the proton of the adjacent amine group in the intermediate species AMH^{2+} for calcimycin. Some studies[48,49] with vesicles have corroborated the trends of our kinetic results. Much slower transport rates by calcimycin have been reported for calcium with negatively charged phospholipids[48] in agreement with large proton interfacial concentrations for surface-charged membranes. The influence of proton concentrations on cation influx into phospholipid vesicles has been correlated to the protonation[49] of the ionophore A-23187.

Let us compare now the kinetic behavior of X-14885A and A-23187. We have collected in Table XII the kinetic parameters we have determined concerning the AM^+ complexes, no kinetic information being available for the faster process of gain or loss of the second ionophore molecule. The ionophore X-14885A will be a kinetically faster ionophore than A-23187, since all the kinetic constants relative to either the formation or the dissociation of AMg^+ and ACa^+ complexes are higher (about 1 order of magnitude). The formation rate constants k_1 are high in agreement with high solvent-exchange rate constants for calcium and magnesium cations.[37] The formation rate constants determined for AMg^+ with both the ionophores are very near the value (8×10^6 mol^{-1} L s^{-1}) obtained for magnesium murexide[37] in the same solvent. These values are far higher than the formation rates of magnesium cryptates in methanol ($\simeq 10^4$ mol^{-1} L s^{-1}).[50] Our results, in agreement with the proposed mechanism by Thomas et al.[12] for the formation of ANi^+ with calcimycin, predict a dissociation interchange model with a rate-limiting step, which is the first-bond formation with the carboxylate oxygen. Both ionophores obey a step by step desolvation mechanism of the cations, which explains the high k_1 values observed. Similarity between the ionophores is a kinetic selectivity for calcium compared to magnesium, all the formation or dissociation steps being

(44) Bolte, J.; Demuynck, C.; Jeminet, G.; Juillard, J.; Tissier, C. *Can. J. Chem.* **1982**, *60*, 981.
(45) Lehn, J. M. *Struct. Bonding* **1973**, *16*, 1.
(46) Caswell, A. H.; Pressmann, B. C. *Biochem. Biophys. Res. Commun.* **1972**, *49*, 292.
(47) Case, G. D.; Vanderkooi, J. M.; Scarpa, A. *Arch. Biochem. Biophys.* **1974**, *162*, 174.
(48) Wun, T. C.; Bittman, R. *Biochemistry* **1977**, *16*, 2080.
(49) Pohl, W. G.; Kreikenbohm, R.; Seuwen, K. *Z. Naturforsch., C: Biosci.* **1980**, *35C*, 562.
(50) Cox, B. G.; van Truong, Ng.; Schneider, H. *J. Am. Chem. Soc.* **1984**, *106*, 1273.
(51) Diebler, H.; Secco, F.; Venturini, M. *J. Phys. Chem.* **1984**, *88*, 4229.
(52) Diebler, H.; Secco, F.; Venturini, M. *J. Phys. Chem.* **1987**, *91*, 5106.
(53) No significant effect of the dichloroacetic buffer was observed in our experimental conditions (total concentration of $CHCl_2COOH = 10^{-2}$ mol L^{-1}).

faster for calcium than for magnesium.

In conclusion, X-14885A behaves like calcimycin as a selective calcium ionophore. The selectivity differences between the ionophores is predominantly of kinetic origin, with faster formation and dissociation rates for calcium complexes than for magnesium. Replacement of the -NHMe group in calcimycin by an -OH group in X-14885A has a drastic effect on the acid-base properties of X-14885A and on the proton-assisted dissociation pathway of its complexes.

Acknowledgment. We gratefully acknowledge the CNRS for financial support. Dr. H. Diebler (Max Planck Institut für biophysikalishe Chemie, Göttingen, RFA) is also thanked for helpful discussions.

Solid-State ^2H NMR Study of Thymidine. Base Rigidity and Ribose Ring Flexibility in Deoxynucleosides

Yukio Hiyama,*[†,‡] Siddhartha Roy,[§,⊥] Jack S. Cohen,[§] and Dennis A. Torchia[‡]

Contribution from the Bone Research Branch, National Institute of Dental Research, and Clinical Pharmacology Branch, National Cancer Institute, National Institutes of Health, Bethesda, Maryland 20892. *Received February 9, 1989*

Abstract: We have investigated the internal motions of the nucleoside thymidine in the solid state by deuterium NMR spectroscopy. The base position was found to be essentially rigid, even at elevated temperatures. On the other hand, T_1 measurements on 2',2''-dideuteriothymidine indicated the presence of small-amplitude motions on the nanosecond time scale. In addition, spin alignment and distorted echo experiments revealed the presence of large-amplitude motion on millisecond to microsecond time scales. This motion is hypothesized to be 2'-endo ↔ 3'-endo interconversion. It was also shown that the large-amplitude motion may be very sensitive to the crystal packing forces.

It has been clear for a while that the three-dimensional conformation of biological macromolecules is the determinant of biological function.[1] A molecule may have more than one such stable conformation available to it. If transitions between such conformations are kinetically possible, then more than one conformation can be utilized for more than one biological task. Thus, a measure of dynamic flexibility (i.e., transitions between different conformations) can provide information about accessible conformations of a biomolecule.

A number of techniques have been employed to measure dynamical properties of molecules.[2] Nuclear magnetic resonance spectroscopy has been widely used to measure motional properties in solution and in the solid state.[3-6] Several types of nuclei can be utilized as probes for measuring dynamics in the solid state. One of the most useful nuclei is ^2H. This quadrupolar nucleus has been used to detect motions in the 10^{-5}-10^{-11}-s range.[7] Recently, spin alignment experiments[8,9] were used to detect motions on very slow time scales. DNA in the cell nucleus spends most of its time in a solidlike environment. There it undergoes many conformational changes, some of which involve a change in conformation of the sugar residues (e.g., B to Z, B to A, etc). Energetics of such transitions have been reported in solution, but very little is known in solid or solidlike states.

We have focused our attention on characterization of the motions of sugar rings of nucleosides in the solid state. In solution, nucleosides are known to interconvert rapidly between 2'-endo and 3'-endo conformations. Such information about ring mobility of nucleosides in the solid state was not available before. Previously we have reported a preliminary study of sugar ring mobility in thymidine and 2'-deoxyguanosine.[10] Here we present a further characterization of such motion in the solid state.

Experimental Section

Thymine-*methyl*-d_3 was purchased from Merck, Sharp and Dohme Isotopes. 2-Deoxyribose 1-phosphate and thymidine phosphorylase were obtained from Sigma Chemical Co. Thymidine phosphorylase was dialyzed twice against 2 L of 0.01 M Tris-*d* and 0.05 M NaCl (pH 7.5) for 2 days, before use. A 10-mL portion of 2-deoxyribose 1-phosphate in water was added to 500 mL of 0.2 M Tris-*d* (pH 7.5) containing 0.05 M NaCl. A 10-mL portion of 0.2 M thymine-*methyl*-d_3 in 0.05 M NaOH was added. This was followed by addition of approximately 300 units of thymidine phosphorylase. Progress of the reaction was monitored by the change in optical density at 295 nm. After the reaction was completed, the reaction mixture was lyophilized, redissolved in water, and purified according to Roy et al.[10] Purity of the sample was checked by UV and ^1H NMR spectra. Since recrystallization of thymidine-*2'-C,2'-C*-d_2 was difficult because of the small amount, all samples for the solid-state NMR work were lyophilized from H_2O or D_2O. Thymidine-*3,3'-O,5'-O*-d_3 was obtained by dissolving thymidine in D_2O and then lyophilizing the solution to remove excess D_2O.

Solid-state ^2H NMR spectra were observed at 38.45 and 76.76 MHz by a home-built[11] and a modified[12] NIC-500 spectrometer, respectively. The 90° pulse length was 2.2 and 2.5 μs at 38.45 and 76.76 MHz. Anisotropic T_2 distortion was measured by changing delay time between the two pulses. Spin alignment echo experiments were performed at 76.76 MHz. The delay time between the first pulse and second pulse, τ_1, was 30 μs, and the delay time between the second pulse and third pulse, τ_2, varied from 500 μs to 100 ms.

Results

Base Rigidity. Figure 1 shows ^2H NMR spectra of thymidine-*methyl*-d_3 at +75 °C (a) and +22 °C (b), which have typical ^2H NMR line shapes for the reorientating methyl group. However,

† Present address: Control Research and Development, Upjohn Pharmaceuticals Ltd., 23 Wadai, Tsukuba 300-42, Japan.
‡ National Institute of Dental Research.
§ National Cancer Institute.
⊥ Present address: Department of Biophysics, Bose Institute, CIT Scheme VII M, Calcutta, 700 054 India.

(1) Anfinsen, C. B.; Haber, E.; Sela, M.; White, F. H., Jr. *Proc. Natl. Acad. Sci. U.S.A.* **1961**, *47*, 1309-1314.
(2) Bayley, P. M., Dale, R. E., Eds. *Spectroscopy and the Dynamics of Molecular Biological Systems*; Academic Press: London, 1985.
(3) *Mobility and function in proteins and nucleic acids*; Ciba Foundation Symposium 93; Pitman Books: London, 1983.
(4) Griffin, R. G. *Methods Enzymol.* **1981**, *72*, 108-174.
(5) Opella, S. J. *Annu. Rev. Phys. Chem.* **1982**, *33*, 533-562.
(6) Torchia, D. A. *Annu. Rev. Biophys. Bioeng.* **1984**, *13*, 125-144.
(7) Spiess, H. W.; Sillescu, H. *J. Magn. Reson.* **1981**, *42*, 381-389.
(8) Spiess, H. W. *J. Chem. Phys.* **1980**, *72*, 6755-6762.
(9) Fujara, F.; Wefing, S.; Spiess, H. W. *J. Chem. Phys.* **1986**, *84*, 4579-4584.
(10) Roy, S.; Hiyama, Y.; Torchia, D. A.; Cohen, J. S. *J. Am. Chem. Soc.* **1986**, *108*, 1675-1678.
(11) Sarkar, S. K.; Sullivan, C. E.; Torchia, D. A. *J. Biol. Chem.* **1983**, *258*, 9762-9767.
(12) Hiyama, Y.; Silverton, J. V.; Torchia, D. A.; Gerig, J. T.; Hammond, S. J. *J. Am. Chem. Soc.* **1986**, *108*, 2715-2723.

0002-7863/89/1511-8609$01.50/0